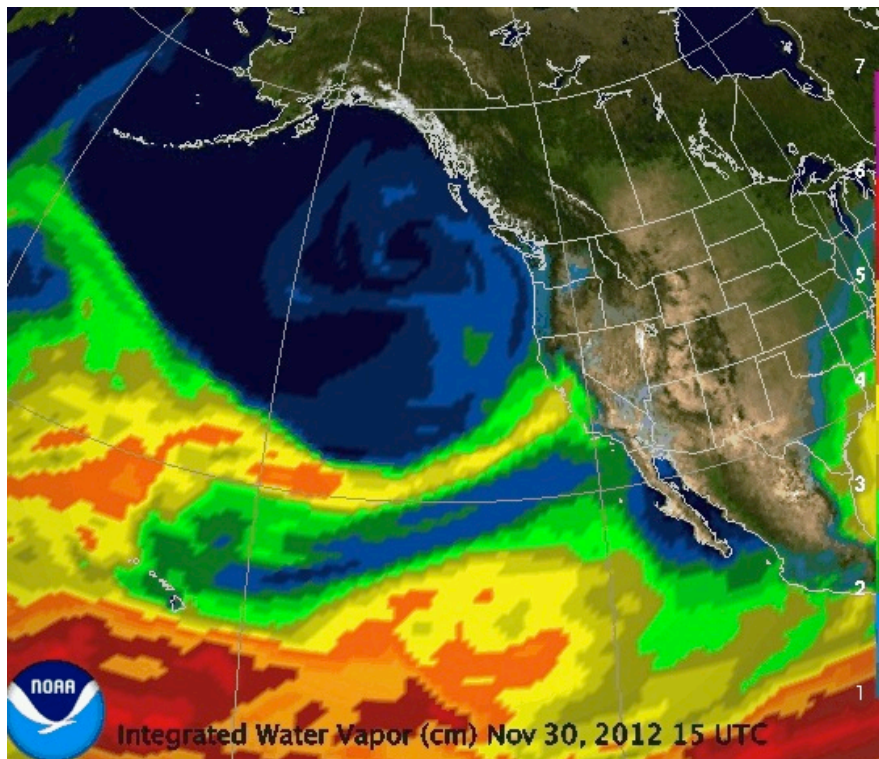


# ASSESSMENT OF THE 2012 GRAVEL/COBBLE AUGMENTATION IN THE ENGLEBRIGHT DAM REACH OF THE LOWER YUBA RIVER, CA IN RESPONSE TO ATMOSPHERIC RIVER FLOODS



An atmospheric river (thin yellow band) feeds torrential rain into northern California on Nov. 30. Image courtesy of NOAA from

<http://blogs.scientificamerican.com/observations/2012/11/30/mysterious-atmospheric-river/>

Prepared for:  
U.S. Army Corps of Engineers  
Sacramento District  
Englebright/Marlis Creek Lakes  
PO Box 6  
1296 Englebright Dam Road  
Smartsville, CA 95977

Prepared by:  
Rocko A. Brown, MS, EIT  
Gregory B. Pasternack, PhD  
University of California, Davis

May 8, 2014

## Abstract

Since 2007 the USACE has been injecting coarse sediment into the Englebright Dam Reach (EDR) of the lower Yuba River (LYR) for spawning habitat rehabilitation. The first injection was in 2007 when ~ 500 short tons were added to the river using a truck-mounted conveyor belt. In 2010, Pasternack (2010) developed a gravel augmentation implementation plan (GAIP) that laid the foundation for future gravel augmentation. The GAIP specified an approximate sediment budget for the reach along with specific geomorphic and ecological goals. In January 2011, the USACE added ~ 5,000 short tons of sediment into the EDR and this addition was extensively monitored. In August of 2012, an additional ~ 5,000 short tons of sediment were added to the river and the status of the site up to December 2012, including chinook spawning utilization, was assessed. Thereafter in November and December of 2012 a moderate flood occurred followed by a smaller flood, both due to an atmospheric river, but then the remainder of the 2013 water year was extremely dry. The two goals of this report were to evaluate the status of gravel/cobble in the EDR as of summer 2013 and explore the fate of the 2012 gravel/cobble injection project in response to these two storms.

The atmospheric river storms that occurred in November and December of 2012 produced two peak discharge events in the EDR that were above the bankfull flow of 5,000 cfs. Only the first storm, which peaked at over 30,000 cfs was of sufficient magnitude to effect channel change in the EDR. TCD and sediment budgeting analyses predicted that erosion of the 2012 gravel injection project with some material remaining upstream. Sediment budgeting and TCD analyses accounted for 82% of the sediment that was injected upstream during the summer of 2012. It was found that a single flood can route gravel deposits a modest distance, but the floods analyzed herein did not route any of the 2012 injection out of the EDR. It appears that most of the sediment injected made it to just above Sinoro Bar. Sediment budgeting for 2007 to the summer of 2013 accounted for 86% (7,625 tons) of the two gravel augmentation projects that have occurred to that point in time. Overall, widespread deposition in the channel has occurred, but some material is also likely leaving the EDR. Given the topographic complexity of the cobble and boulder strewn riverbed, it is very difficult to determine if unaccounted for sediment is in the bed or leaving the reach, but no sizable deposits are observed in the Narrows Reach at this time.

Citation: Brown, R.A. and Pasternack, G.B. 2014. Assessment Of The 2012 Gravel/Cobble Augmentation In The Englebright Dam Reach Of The Lower Yuba River, Ca In Response To Atmospheric River Floods. Prepared for the U.S. Army Corps of Engineers, Sacramento District. University of California at Davis, Davis, CA.

## **Acknowledgements**

This project was sponsored by the United States Army Corps of Engineers under Cooperative Ecosystem Studies Unit Award # W912HZ-11-2-0038. This project was also supported by the USDA National Institute of Food and Agriculture, Hatch project number #CA-D-LAW-7034-H.

The authors thank Sean W. Smith with construction and implementation support and lessons learned; Doug Grothe for contracting and coordination.

## Preface

This report seeks to understand how the 2<sup>nd</sup> gravel injection of 5,000 tons in the Englebright Dam Reach of the lower Yuba River responded to two atmospheric river floods that occurred relative to the Army Corps' 2010 Gravel Augmentation Implementation Plan. A report dated December 15, 2012 presented the finding for the period of November 1, 2007 to November 1, 2011. During that time there was a small pilot cobble/gravel injection in late November 2007 and a substantial one in November 2010 to January 2011. The second report dated September 1, 2013 covers the period November 1, 2011 to December 1, 2012. During this latest interval there was a gravel/cobble injection during July to August 2012. After this injection, two atmospheric river storms produced moderate runoff volumes from the watershed and the effect of these floods on gravel transport and storage is assessed in this report.

This report duplicates many of the methods and analyses from the previous report, so several sections have been carried over from the previous year's monitoring report. In some cases minor typographical errors and citation errors have been fixed. These sections are mostly background information and methods that apply to both years. These sections will have an asterisk (\*) next to the section heading so that readers who are familiar with the prior year's results can skip these sections and focus on new results.

# Table of Contents

Abstract.....	ii
Acknowledgements .....	iii
Preface	iv
Table of Contents .....	v
List of Tables .....	vii
List of Figures .....	viii
1.0 Introduction.....	1
2.0 Goals and Objectives.....	1
2.1. Peak Flow Hydrology after Injection.....	2
3.0 Post-Project Data Collection.....	3
3.1. Topography and Bathymetry.....	3
3.2. Topographic Map Construction .....	4
3.3. Google Earth Aerial Imagery .....	4
4.0 Data Analysis Methods.....	5
4.1. Areal Extent of Gravel/Cobble Deposits from Imagery.....	5
4.2. Topographic Change Detection By DEM Differencing.....	5
4.2.1. TCD Components .....	5
4.2.2. TCD Production Workflow*.....	6
4.2.3. Volume and Weight Gravel/Cobble Budgeting* .....	8
5.0 Results .....	9
5.1. Deposition Polygons From Image Analysis.....	9
5.2. Survey and Instrumentation Error (SIE) Functions .....	9
5.3. TCD Analyses.....	13
5.3.1. Fall 2012 to Summer 2013 TCD.....	13
5.3.2. 2007 to Summer 2013 TCD.....	17
5.4. Sediment Budgeting .....	21
5.4.1. Sediment Budget for Fall 2012 to Summer 2013.....	21
5.4.2. Overall Sediment Budget from 2007-2013.....	22
6.0 The Role of Deer Creek on Sediment Storage in the EDR .....	23
7.0 Conclusions .....	26

8.0	References .....	28
-----	------------------	----

## List of Tables

Table 1. Ranges of applicability for SIE functions with $R^2$ values for the upstream area of the October 2012 data .....	12
Table 2. Ranges of applicability for SIE functions with $R^2$ values for the upstream area for the summer 2013 data .....	12
Table 3. Ranges of applicability and SIE functions with $R^2$ values for the downstream area for the fall 2012 data.....	13
Table 4. Ranges of applicability for SIE functions with $R^2$ values for the downstream area for the summer 2013 data.....	13
Table 5. Upstream and downstream volumes of erosion and deposition for the Fall 2012 to Summer 2013 epoch after accounting for uncertainty.....	15
Table 6. Upstream and downstream volumes of erosion and deposition for the 2007 to Summer 2013 epoch.....	18

## List of Figures

Figure 1. Mean daily discharge recorded at the Smartsville gage ( <a href="http://cdec.water.ca.gov">http://cdec.water.ca.gov</a> ; YRS) during the period between November 2012 and January 2013. ....	2
Figure 2. Survey limits and collected points in summer 2013.....	3
Figure 3. Polygons outline areas of gravel deposition that were discernible using the Google Earth imagery taken in May of 2013 and RTK data collected during the summer of 2013.....	9
Figure 4. Plots of the elevation error and local surface elevation variation ( $\sigma Z$ ; LEFT) and standard deviation of elevation error ( $\sigma\Delta Z$ ) versus the local surface elevation variation ( $\sigma Z$ ; RIGHT) for for the upstream area of the fall 2012 data. ....	10
Figure 5. Plots of the elevation error and local surface elevation variation ( $\sigma Z$ ; LEFT) and standard deviation of elevation error ( $\sigma\Delta Z$ ) versus the local surface elevation variation ( $\sigma Z$ ; RIGHT) for the upstream area for the summer 2013 data.....	11
Figure 6. Plots of elevation error and local surface elevation variation ( $\sigma Z$ ; LEFT) and standard deviation of elevation error ( $\sigma\Delta Z$ ) versus local surface elevation variation ( $\sigma Z$ ; RIGHT) for the downstream area of for the fall 2012 data.....	11
Figure 7. Plots of the elevation error and local surface elevation variation ( $\sigma Z$ ; LEFT) and standard deviation of elevation error ( $\sigma\Delta Z$ ) versus the local surface elevation variation ( $\sigma Z$ ; RIGHT) for for the downstream area for the summer 2013 data. ....	12
Figure 8. Upstream injection area patterns of erosion and deposition for the Fall 2012 to Summer 2013 epoch at the 95% confidence limit.....	15
Figure 9. Downstream injection area patterns of erosion and deposition for the Fall 2012 to Summer 2013 epoch at the 95% confidence limit. ....	16
Figure 10. Erosion associated with the fall 2012 to summer 2013 TCD analysis (in red) and the areal extent (blue outline and transparent fill) of deposition associated with prior TCD analyses from 2011 to fall 2012. 77% of erosion was associated with areas that previously had gravel deposition.....	17
Figure 11. Elevation change histogram for the upstream area (left) and downstream area (right) for the Fall 2012 to Summer 2013 epoch. ....	17
Figure 12. Upstream injection area patterns of erosion and deposition for the 2007 to Summer 2013 epoch at the 95% confidence limit.....	19

Figure 13. Downstream area TCD predicted patterns of erosion and deposition for the 2007 to Summer 2013 epoch at the 95% confidence limit. .... 20

Figure 14. Elevation change histogram for the upstream area (left) and downstream area (right) for the 2007 to summer 2013 epoch..... 21

Figure 15. Hydrographs of the Yuba River at the Smartsville gage (YRS) and for Deer Creek (DCS) for the 2005/2006 NYE storm. .... 25

Figure 16. Hydrographs of the Yuba River at the Smartsville gage (YRS) and for Deer Creek (DCS) for the atmospheric river floods of Nov./Dec. 2012 studied in this report. .... 26

## **1.0 Introduction**

The USACE has been injecting coarse sediment into the Englebright Dam Reach (EDR) of the lower Yuba River for spawning habitat rehabilitation. The first injection was in 2007 when ~ 500 short tons were added to the river using a truck-mounted conveyor belt (Pasternack, 2009). In 2010, Pasternack (2010) developed a gravel augmentation implementation plan (GAIP) that laid the foundation for future gravel augmentation. The GAIP specified an approximate sediment budget for the reach along with specific geomorphic and ecological goals. In January 2011, the USACE added ~ 5,000 short tons of sediment into the EDR and this addition was extensively monitored (Brown and Pasternack, 2012). In August of 2012, an additional ~ 5,000 short tons of sediment were added to the river and the status of the site up to December 2012, including chinook spawning utilization, was assessed (Brown and Pasternack, 2013). Thereafter a moderate flood occurred followed by a smaller flood, both due to an atmospheric river, but then the remainder of the 2013 water year was extremely dry. This report presents the findings about how the EDR changed in response to that flood, including assessment of what happened to the sediment injected in August 2012.

## **2.0 Goals and Objectives**

The overall goals of this study were to evaluate the status of gravel/cobble in the EDR as of summer 2013 and explore the fate of the 2012 gravel/cobble injection project in response to two winter storms that occurred in November and December of 2012 associated with atmospheric rivers. Atmospheric rivers are narrow bands of water vapor several miles long and about a mile high in the sky that are generated in the Pacific Ocean. They've historically been a source of precipitation in California and as well as a dominant hydrologic driver in the Yuba River basin. The 2012 gravel injection project and subsequent topographic mapping were completed before these storms occurred. Because there were no other major storms the remainder of the 2013 water year, the opportunity exists to analyze the fate of the 2012 gravel injection from these two events alone as well as to summarize the status of the reach as of summer 2013.

## 2.1. Peak Flow Hydrology after Injection

Brown and Pasternack (2013) covered the period of November 1, 2011 to December 1, 2012. This report starts with the fall 2012 topographic data set and goes through the summer of 2013 when post flood mapping was completed. Both storms occurred in a short period between the two mapping campaigns, the first in late November and the second in late December (Figure 1). Pasternack (2008) reported that in the most constricted location upstream of the 2010-2011 injection point, a state of “partial transport” in which overrepresented finer gravels are scoured disproportionately begins at ~ 10,000 cfs and full mobility of the riverbed begins at ~ 25,000 cfs (see figure 108 of Pasternack, 2008). Therefore, only the first storm is likely to have contributed to sediment transport and channel change for this period.

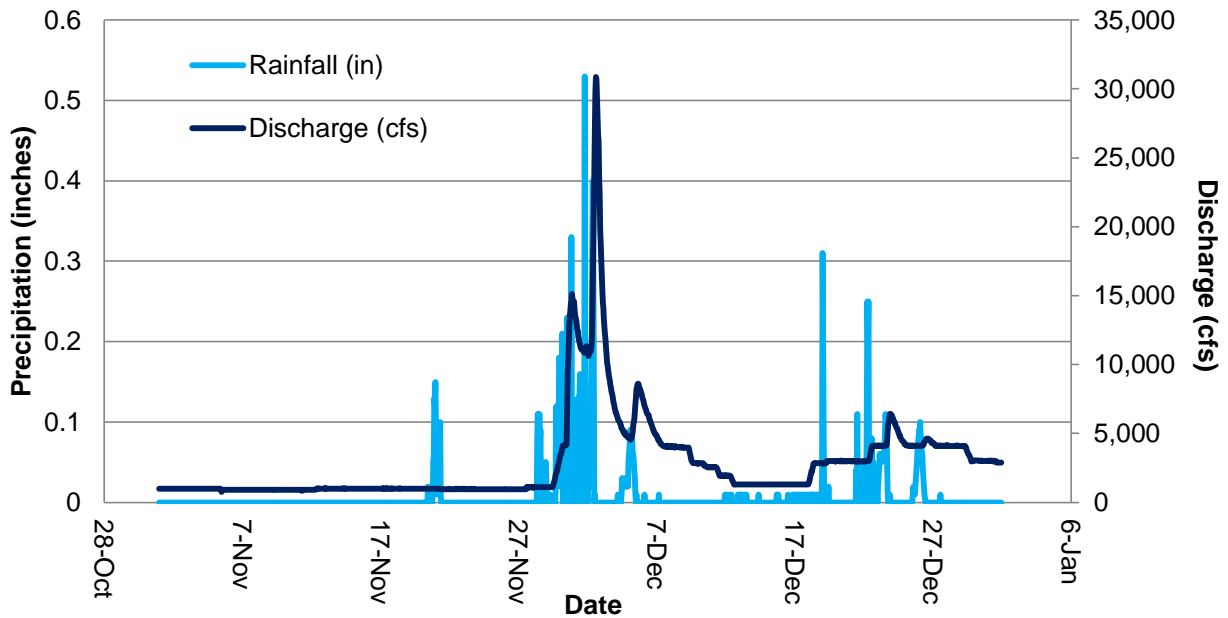


**Figure 1. Mean daily discharge recorded at the Smartsville gage (<http://cdec.water.ca.gov>; YRS) during the period between November 2012 and January 2013.**

### 3.0 Post-Project Data Collection

Data collection and project monitoring took place in the summer after the 2012 cobble/ravel injection was completed. Topographic and bathymetric data was collected following methods outlined in the last two years' monitoring reports.

#### 3.1. Topography and Bathymetry

The baseline EDR topographic map for analysis of channel change and sediment-budget computation dates to a period from 2005-2007 when EDR was mapped (Pasternack, 2008). The upstream gravel injection deposit was mapped in October 2012 as described in Brown and Pasternack (2013). New topographic and bathymetric surveys took place over several days during June through July of 2013. One additional effort took place in early September to fill in gaps from the prior months. Existing topographic ground control for the EDR was used that is tied into the State Plane California Zone 2 coordinate system in units of feet with NAD 1983 and NAVD88 horizontal and vertical datums, respectively. Terrestrial (and some wadable aquatic) surveying was done using a Leica TPS1200 total station and a Trimble R7 RTK GPS to map emergent and shallow gravel. Bathymetric mapping where depth > 1.0' was performed using the same methodology as last year where a kayak was outfitted with an echosounder and RTK GPS. The approach used involved a Sonarmite echosounder (Seafloor Systems, Inc., Folsom, CA) coupled with a Trimble R7 RTK GPS for geographic positioning mounted onto a kayak.

All areas within the study reach were surveyed with the exception of the area immediately upstream and the center of the rapid downstream of the USGS gaging station due to safety reasons and problems with air bubbles confounding the echosounder. For the summer 2013 survey the total number of points collected was 48,546, of which 48,527 were used in the analyses over an area of 400,374 ft<sup>2</sup>, yielding a point density of 0.12 points per ft<sup>2</sup>, which is ~1.3 points per m<sup>2</sup> (Fig. 2).

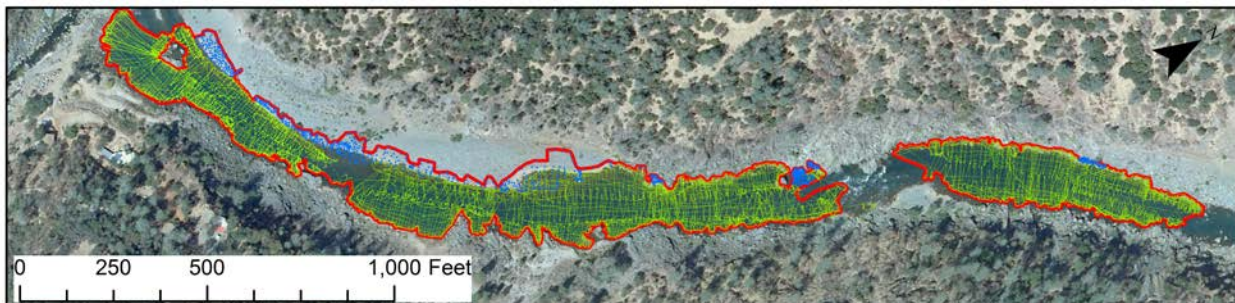


**Figure 2. Survey limits and collected points in summer 2013.**

### **3.2. Topographic Map Construction**

Because this study evaluated time-dependent changes in topography, it was necessary to create topographic maps for the two times considered. The times considered here are fall 2012 (surveyed in October after the injection), and summer 2013 (post flood conditions surveyed in June and July of 2013). The data available from each time were used to map the surveyed areas, not to produce a complete map of the whole EDR for each time. The baseline map for October 2012 was previously produced and reported by Brown and Pasternack (2013); it is a complete map of EDR including hillsides.

In addition to these partial maps, a new comprehensive map for the whole EDR was made blending the most recent observations available at each location; some locations, especially the hillsides, continue to use older data from 1999 and 2005-2007, because they are out of the channel and not a priority to re-map. Because it remains infeasible to map the center of the rapid below the USGS gaging station (just as it was previous efforts), it was necessary to use breaklines and artificial contours to create the best representation as possible for that small but important location that acts as a hydraulic control on channel upstream of it. This new complete EDR map was used solely to assess the fate of the 2012 injection in response to the atmospheric floods.

Topographic maps and associated digital elevation models (DEMs) were made in ArcGIS 10 using 3D Analyst. For each survey, boundary polygons were drawn around the new data collected at that time. Then a triangulated irregular network (TIN) was created using the points in the boundary polygons and the boundary itself as a hard clip. Finally, the TIN was converted to a 3'x3' raster for that point in time. A similar procedure was used to create a TIN and 3'x3' raster of the new complete EDR map.

### **3.3. Google Earth Aerial Imagery**

Google Earth © had imagery dated 5/2/2013 where lighter colored gravel deposits could be seen. To utilize this data source, 19 zoomed in frames of the site were exported at varying resolutions. Then, these 19 images were mosaicked using Agisoft© as described above. Finally, the composite image was also rectified in ArcGIS© using known targets.

## **4.0 Data Analysis Methods**

### **4.1. Areal Extent of Gravel/Cobble Deposits from Imagery**

A first step in assessing the spatial position of the gravel/cobble deposits was to determine areas of deposition of augmented gravels from Google Earth imagery. To do this, the mosaic was processed in ArcGIS 10 using the image analysis toolbar to help visualize the deposits better. Adjustment of image brightness and contrast provided the best way to isolate patches of new gravel. Once areas were identified their spatial extents were mapped by creating a polygon shapefile. The final Google Earth image has a cell size of 0.9 ft. Because this image was of poorer quality when mosaicked, the gravel deposits were outlined in Google Earth and then converted to a shapefile for use in ArcGIS. Lastly, while topographic surveying occurred, some RTK data was also collected on river right on fresh gravel deposits. These points were converted to polygons and the total area added to the image analysis.

### **4.2. Topographic Change Detection By DEM Differencing**

Per the GAIP, the test for design hypothesis one is an evaluation of topographic change from difference of DEMs (Wheaton et al, 2010a,b; Carley et al., 2012). In simplest terms, a DEM difference is just the subtraction of one topographic map (i.e. a raster map) from another with the resulting difference indicating the locations and magnitudes of landform change. The map of topographic change itself may be represented by a DEM, so it is termed the DEM of Difference (DoD). However, topographic maps have uncertainties in them that people normally do not think much about. When a DoD is produced, it not only has the errors from each source map, but also the errors of propagation through the mathematics. As a result, it is crucial to characterize DoD uncertainty instead of relying on analysis of a raw DoD. Topographic change detection (TCD) by DoD analysis including uncertainty is a rapidly progressing technique for monitoring and understanding rivers (Wheaton et al., 2010a,b; Carley et al., 2012). For this study, three sets of topographic data were used in four topographic change scenarios to evaluate changes in topography using the method developed by the RMT for use on the lower Yuba River (Carley et al., 2012).

#### **4.2.1. TCD Components**

Because of the significant role of the rapid downstream of the USGS gaging station in serving as a topographic control on channel hydraulics, EDR was divided into two sections for TCD by DOD analysis at this location, segregated by a red line in the results

figures. The upstream area (injection zone to crest of rapid) was isolated to assess sequential fill and scour periods that occurred between the October 2011 and October 2012 surveys. The downstream area (rapid crest to Narrows Gateway entrance) was isolated to analyze the overall net change in the river between the October 2011 and October 2012 surveys. Further, both areas were also assessed between the 2007 and October, 2012 survey as well to evaluate the status of gravel injections in the study reach.

#### **4.2.2. TCD Production Workflow\***

The Carley et al. (2012) method of accounting for uncertainty with geomorphic change detection was once again utilized to perform topographic change detection and analysis with an additional improvement related to generating a survey and instrumentation error (SIE) function. This method is based on the idea that locations where there is a lot of topographic variation in the raw point data for a topographic map are the ones that are most uncertain (Heritage et al., 2009). Consequently, the more variation a location has, the higher the bar has to be to consider raw DoD values as real as opposed to an artifact of map errors. Topographic variation stems from measurement error as well as natural sharp features (e.g. steep banks, boulder clusters, and sedimentary bars). By focusing on the existence of topographic variation regardless of its cause, the method is less sensitive to expert-based decisions as to potential native sources of topographic error.

A departure from the analysis of Brown and Pasternack (2012) was the development and use of data driven survey and instrumentation error (SIE) functions. The methodology developed by Milan et al. (2011) was used to achieve this. This method develops data specific SIE functions for each survey period and extent based on the raw surveyed point elevations,  $Z_S$ , the raster interpolated elevations,  $Z_R$ , the local surface elevation variation,  $\sigma_Z$ , and the standard deviation of elevation variation,  $\sigma_{\Delta Z}$ . The analysis involved the following steps in ArcGIS 10 adapted from Milan et al. (2011):

1. Convert final topographic TIN for each time point to 1-ft raster and clip to TCD extents
2. Convert each raster to points, creating the raster elevation  $Z_R$  dataset.
3. Create a standard deviation raster with a 3-ft grid, producing the  $\sigma_Z$  data set.
4. Merge all raw surveyed point data sets so that they have the same field for surveyed elevation values,  $Z_S$ .
5. Spatial join  $Z_S$  with  $Z_R$

6. Calculate  $\Delta Z = Z_R - Z_S$
7. Sample the  $\sigma_Z$  data set to the point file with  $Z_S$  with  $Z_R$ .
8. Make scatterplot of  $\Delta Z$  vs.  $\sigma_Z$
9. Aggregate  $\Delta Z$  values within 0.25' intervals of  $\sigma_Z$  and compute  $\sigma_{\Delta Z}$  for each bin.
10. Plot  $\sigma_{\Delta Z}$  vs  $\sigma_Z$  and fit the best trendline to that possible. The trendline is the SIE function needed.

With an SIE function for each survey epoch and TCD extent, implementation of the Carley et al. (2012) method used in this study involved the following steps in ArcGIS 10:

1. Create a uniform  $\{x,y\}$  point grid with 1' point spacing.
2. Elevate the 1' point grid using the topographic data for each map to create oversampled topographic point datasets for  $\{x,y,z\}_{time1}$  and  $\{x,y,z\}_{time2}$  that capture all available topographic information in the source DEMs.
3. For each 1'  $\{x,y,z\}$  topographic dataset, create a raster of standard deviation (SD) of point elevation with a 3'x3' cell size (yielding nine points per cell in the statistical computation).
4. Apply the appropriate survey and instrument error (SIE) empirical equation to the SD rasters to obtain the SIE raster for each topographic map.
5. Produce a Level of Detection (LoD) grid that combines the two SIE rasters into a single error raster using the t-value for 95 % confidence (1.96) and the statistical equation for error propagation given by:

$$LoD = t\sqrt{(SIE_{time1})^2 + (SIE_{time2})^2}$$

6. Create the raw DoD raster with a 3'x3' cell size.
7. Create separate deposition and erosion rasters using the "Con" function in the ArcGIS raster calculator.
8. Remove the LoD from each raster by subtracting it from the deposition-only raw DoD and adding it to the erosion-only raw DoD.
9. Create spatial coherence polygons to clip deposition and erosion rasters.
  - a. Con statements were used to turn deposition and erosion rasters into presence/absence polygons.
  - b. The area of each erosion and deposition polygon was calculated.
  - c. A minimum threshold of 100 ft<sup>2</sup> (~9 raster cells) was used to distinguish coherent change.

- d. The original deposition and erosion rasters were clipped to exclude the areas of change below the size threshold.
10. Clip to lowest extent of data set survey limits.

An additional modification to the TCD procedure and final result in this report compared to the previous one was that the exclusion of a uniform threshold for all surveys was not utilized because the SIE functions capture this aspect of the data intrinsically. The uniform exclusion had been +/- 0.16 ft, but it is not necessary with the new procedure.

#### **4.2.3. Volume and Weight Gravel/Cobble Budgeting\***

Once a final DoD raster with a 95% confidence was developed it was necessary to quantify erosion and deposition volumetrically and by weight. To do this, the volume of topographic change for each raster cell was determined by multiplying each cell's change value by the cell's area (3'x3'). This was performed separately for erosion and deposition. Converting volume to mass required an estimate of gravel/cobble bulk density as present in the river. For this study, we used a value of 110 lbs/ft<sup>3</sup> that came from five experimental bucket tests on gravel density performed at a quarry as material was stockpiled for a gravel augmentation on the Mokelumne River (Merz et al., 2006). Given this bulk density value, the conversion from ft<sup>3</sup> to short tons involved multiplying the volume by the bulk density and dividing by the conversion factor of 2,000 lbs per short ton.

The final polygon for gravel deposition from the images and the RTK data were also used to estimate fill volumes outside of what the TCD analysis accounted for. To do this, the final TCD deposition area was subtracted from the image/RTK based polygon to obtain the area not accounted by TCD. To convert this area to a volume we assumed a fill thickness of 0.18 feet, consistent with the lower limit of the SIE functions.

## 5.0 Results

### 5.1. Deposition Polygons From Image Analysis

A very low-resolution version of the final imagery mosaic is shown in Figure 3 with areas of visually discernible gravel deposits enclosed in blue. A larger digital map is available upon request. The areas shown were what could be visually identified as gravel deposits from this year's injection, as well as last year's, that matched the composition of injected gravels. For the area upstream of the rapid the total area was 44,213 ft<sup>2</sup> of which 28,300 (64%) is associated with the 2013 gravel injection project that occurred two months before the image was taken. For the Google Earth image and RTK data the total area of gravel deposition was 114,855 ft<sup>2</sup>, which is 24% of the wetted area at 855 cfs from Narrows 1 to the confluence of Deer Creek at the study limit.



**Figure 3. Polygons outline areas of gravel deposition that were discernible using the Google Earth imagery taken in May of 2013 and RTK data collected during the summer of 2013.**

### 5.2. Survey and Instrumentation Error (SIE) Functions

In this study, local SIE functions were created for the EDR using the method of Milan et al. (2011), which is a more sophisticated and more certain method. Since there was one epoch investigated and two data sets for each epoch, then to compare each against each other meant that four total SIE functions were needed. Each SIE function is dependent on the standard deviation of elevation ( $\sigma_z$ ) and the error from interpolation ( $\Delta z$ ) plots of these two variables are provided along with the final SIE functions. These functions may be used in future reports or new functions can be developed each time. For the TCD epochs that rely on 2007 topographic data the SIE functions are presented in last year's monitoring report (Brown and Pasternack, 2012).

All of the plots of local surface elevation variation versus elevation error illustrate that as the variability of surface increases so does the range of elevation error (Figs. 4-8),

consistent with Milan et al. (2011). In fitting a trend model to the binned standard deviation of elevation error linear and polynomial functions were iteratively adjusted to determine trends that maximized  $R^2$  values (Tables 1-4). For values outside the binned local surface elevation linear models were assumed. This was done because it was thought to be more conservative than reducing the SIE's to zero outside of data limits. For the fall 2012 data both upstream and downstream SIE functions showed increases in the standard deviation of elevation error with local surface variability but did not decline after peaking (Figs. 4,6). In contrast the summer 2013 SIE functions showed declines in the standard deviation of elevation error when the local surface variability peaked (Figs. 6,8). In comparing the two upstream SIE functions the local surface variation was much lower for the as-built gravel injection topography compared to the eroded state that was recorded in the summer of 2013 (Figs. 4,5). This is a reasonable outcome as the topography of the gravel injection would be undeniably smoother than the irregular and boulder bathymetry of the injection location. Similarly, the downstream summer 2013 SIE function had more local surface variability than the fall 2012 SIE function (Figs. 6,7).

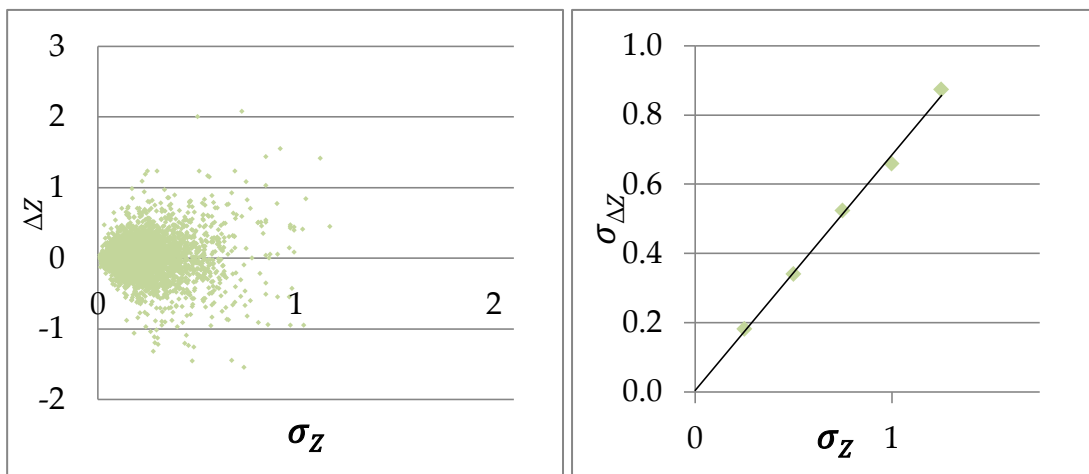


**Figure 4. Plots of the elevation error and local surface elevation variation ( $\sigma_Z$ ; LEFT) and standard deviation of elevation error ( $\sigma_{\Delta Z}$ ) versus the local surface elevation variation ( $\sigma_Z$ ; RIGHT) for for the upstream area of the fall 2012 data.**

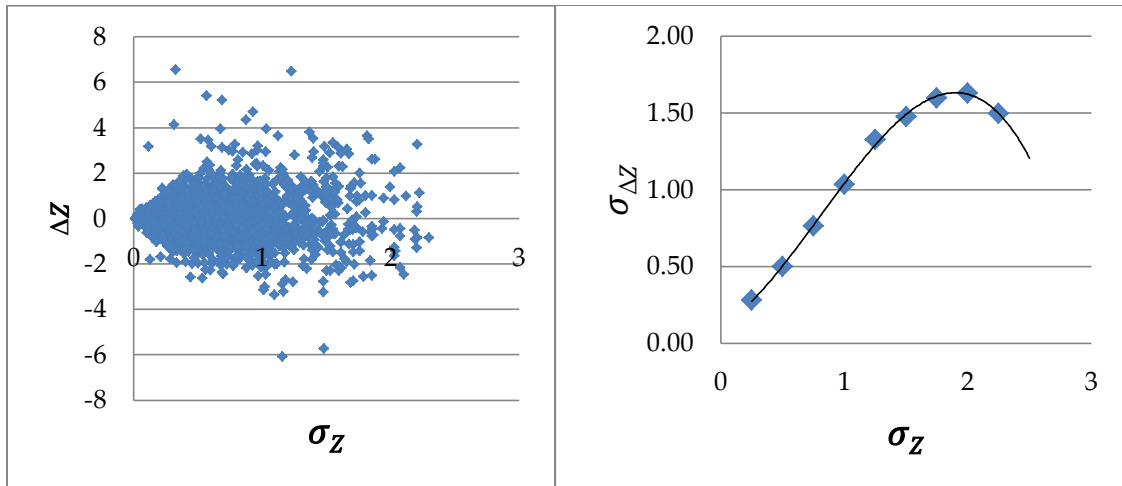


**Figure 5. Plots of the elevation error and local surface elevation variation ( $\sigma_Z$ ; LEFT) and standard deviation of elevation error ( $\sigma_{\Delta Z}$ ) versus the local surface elevation variation ( $\sigma_Z$ ; RIGHT) for the upstream area for the summer 2013 data.**

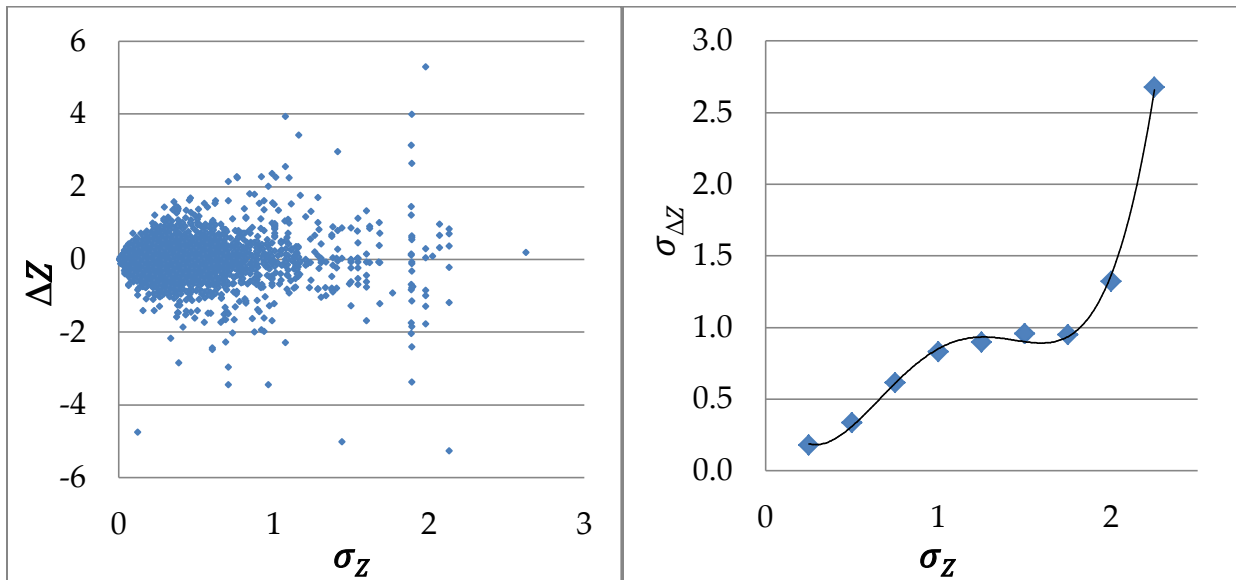


**Figure 6. Plots of elevation error and local surface elevation variation ( $\sigma_Z$ ; LEFT) and standard deviation of elevation error ( $\sigma_{\Delta Z}$ ) versus local surface elevation variation ( $\sigma_Z$ ; RIGHT) for the downstream area of for the fall 2012 data.**

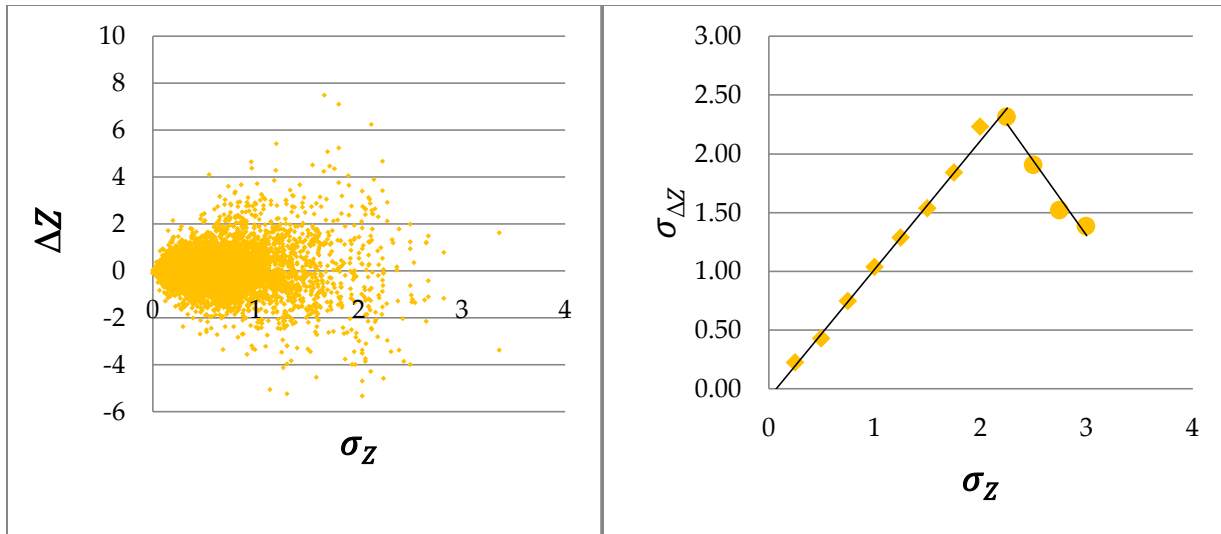


**Figure 7. Plots of the elevation error and local surface elevation variation ( $\sigma_Z$ ; LEFT) and standard deviation of elevation error ( $\sigma_{\Delta Z}$ ) versus the local surface elevation variation ( $\sigma_Z$ ; RIGHT) for for the downstream area for the summer 2013 data.**

**Table 1. Ranges of applicability for SIE functions with  $R^2$  values for the upstream area of the October 2012 data**

Range	SIE Function	$R^2$
0 -0.25	$y = 0.18$	1
0-1.75	$y = 0.6811x + 0.0047$	0.9961
>1.75	$y = 0.87$	1

**Table 2. Ranges of applicability for SIE functions with  $R^2$  values for the upstream area for the summer 2013 data**

Range	SIE Function	$R^2$
0 - 0.25	$Y=0.28$	1
0.25 - 2.25	$y = -0.307x^3 + 0.7437x^2 + 0.498x + 0.1074$	0.99
> 2.25	$Y=1.50$	1

**Table 3. Ranges of applicability and SIE functions with R<sup>2</sup> values for the downstream area for the fall 2012 data**

Range	SIE Function	R <sup>2</sup>
0 - 0.25	y = 0.18	1
0.25 - 2.5	$y = 1.5053x^4 - 6.3119x^3 + 8.5432x^2 - 3.5096x + 0.6244$	0.9722
>2.5	y = 2.68	1

**Table 4. Ranges of applicability for SIE functions with R<sup>2</sup> values for the downstream area for the summer 2013 data**

Range	SIE Function	R <sup>2</sup>
0 - 0.25	y=0.22	1
0.25 -2.25	1.0959x-0.0771	0.9949
2.25-3	-1.2676x+5.106	0.9594
>3	Y=1.38	1

### 5.3. TCD Analyses

Results of topographic change detection come in the form of final adjusted DoD rasters where the LoD for each pixel was subtracted out. Final DoD rasters exist for upstream and downstream areas as well as for two different epochs for both upstream and downstream. Summaries of the results were in the form of tabular amounts, spatial plots, and elevation change histograms for erosion and deposition. All results reported in this section are in units of short tons, as previously defined and explained in section 4.2.

#### 5.3.1. Fall 2012 to Summer 2013 TCD

The upstream TCD analysis yielded 3,129 tons of erosion and 162 tons of deposition for this epoch (Table 5). In addition, 360 tons of erosion and 133 tons of deposition were detected and estimated from the aerial photographs in the river, yielding a net of 3,194 tons of erosion for this epoch. While a spatial coherence filter of 100 ft<sup>2</sup> was implemented, some areas of erosion appear patchy and associated with bank roughness elements such as large boulders and bedrock outcrops on the channel edge and in the

center of the channel. Erosion was also predominantly low magnitude, with 50% and 75% of all erosion cells being less than 2 and 1 ft, respectively. Predicted deposition was focused on river left, but there were also some patches of channel fill at the downstream limit of this TCD analysis located upstream of emergent boulders and bedrock outcrops. Deposition was of much less magnitude than erosion with 50% and 75% of the deposition was less than 0.4 and 0.65 ft (Figure 11).

The TCD analysis for the downstream area predicted 1,116 tons of erosion and 845 tons of deposition, yielding a net of 271 tons of erosion (Table 5). In addition, the image analysis yielded 336 tons of deposition, producing a net of 66 tons of deposition. Statistically significant areas of deposition occurred through the first half of the downstream section on river right where a long deposit formed that is also visible in the images (Figure 9). Adjacent to this area on river left the TCD analysis predicted erosion that was associated with bedrock outcrops. Below this long band of deposition the primary areal response was erosion with deposition being interspersed. In this lower area of the downstream TCD section it appeared that much of the change was too low to be predicted given the LOD. Overall, the topographic change histogram had an even spread centered on erosion on the 0 to -0.5 foot bin (Figure 14). Most erosion was low magnitude change as 75% and 50% of erosion was less than 0.16 and 0.37 feet, respectively. Deposition was of a slightly higher magnitude with 75% and 50% was less than 0.8 and 0.5 feet, respectively. Because erosion was low magnitude it is possible that prior sediments injected were eroded before being replaced due to the relatively short flood season. For the areas that experienced erosion 77% were associated with deposition from the prior two year's TCD analysis (Figure 10). This means that most of the predicted erosion was associated with deposition from prior gravel augmentation.

The patterns of downstream erosion and deposition are peculiar because overall the net change is very low, but there are two somewhat different responses in the downstream area. Why did erosion occur more towards the lower half with a depositional band towards the upper half of the downstream TCD area? There was only one major storm with flows much greater than bankfull during the study period. It is possible that during the rising limb of this event the upstream material that was injected during 2012 became entrained with significant sediment transport. Because the duration was relatively low, and only one major event occurred, the gravel essentially stalled out at the middle of the downstream section as the hydrograph receded. Sediments that eroded below this point were associated with gravel deposited in prior years. Once again, because the storm duration was short, and only one event occurred, it is hypothesized that material in transport upstream could not replenish the areas that eroded towards the lower end of the downstream section.

**Table 5. Upstream and downstream volumes of erosion and deposition for the Fall 2012 to Summer 2013 epoch after accounting for uncertainty.**

	Upstream			Downstream		
	Erosion (tons)	Deposition (tons)	Net (tons)	Erosion (tons)	Deposition (tons)	Net (tons)
2012 Fall - 2013 Summer	-3129	162		-1116	845	
Images/RTK	-435	175		NA	240	
Net	-3564	337	<b>-3227</b>	-1116	1085	<b>-31</b>

Total Change (erosion + deposition) 3,901

2,201

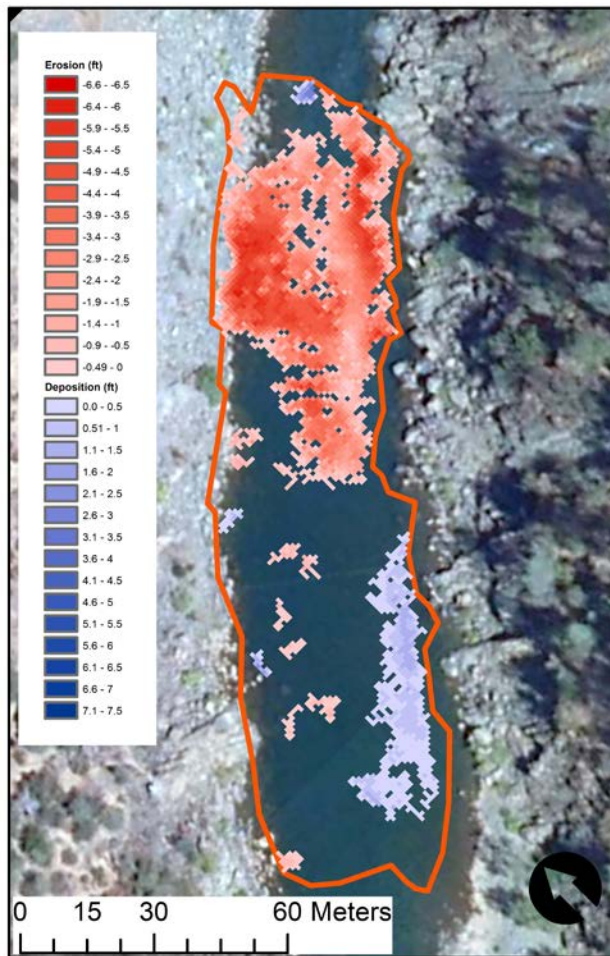


**Figure 8. Upstream injection area patterns of erosion and deposition for the Fall 2012 to Summer 2013 epoch at the 95% confidence limit.**

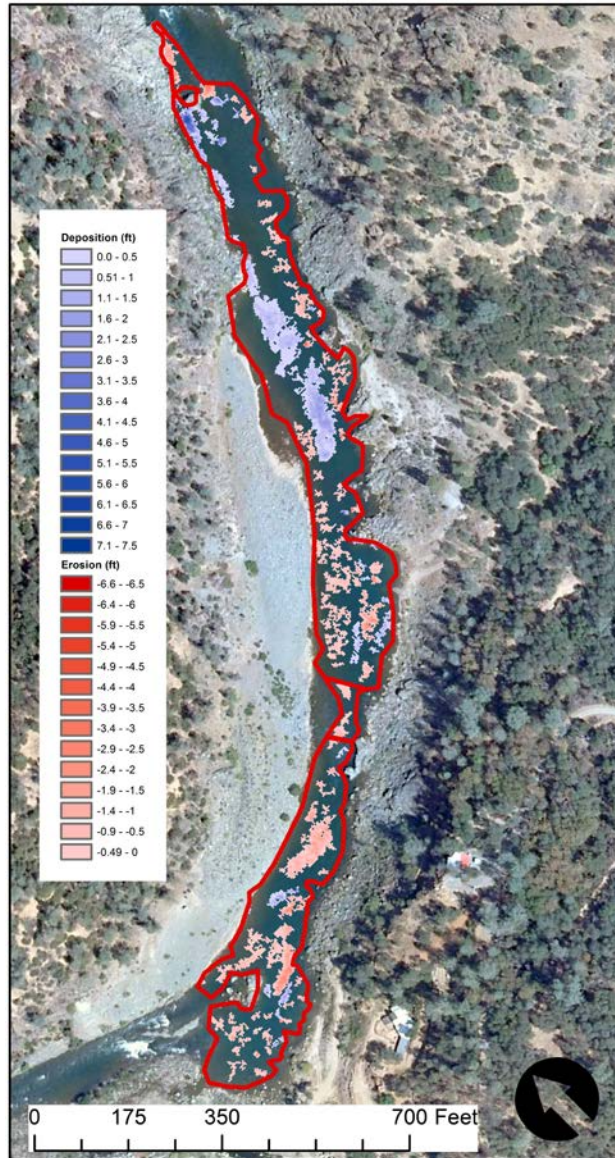


**Figure 9. Downstream injection area patterns of erosion and deposition for the Fall 2012 to Summer 2013 epoch at the 95% confidence limit.**



**Figure 10. Erosion associated with the fall 2012 to summer 2013 TCD analysis (in red) and the areal extent (blue outline and transparent fill) of deposition associated with prior TCD analyses from 2011 to fall 2012. 77% of erosion was associated with areas that previously had gravel deposition.**

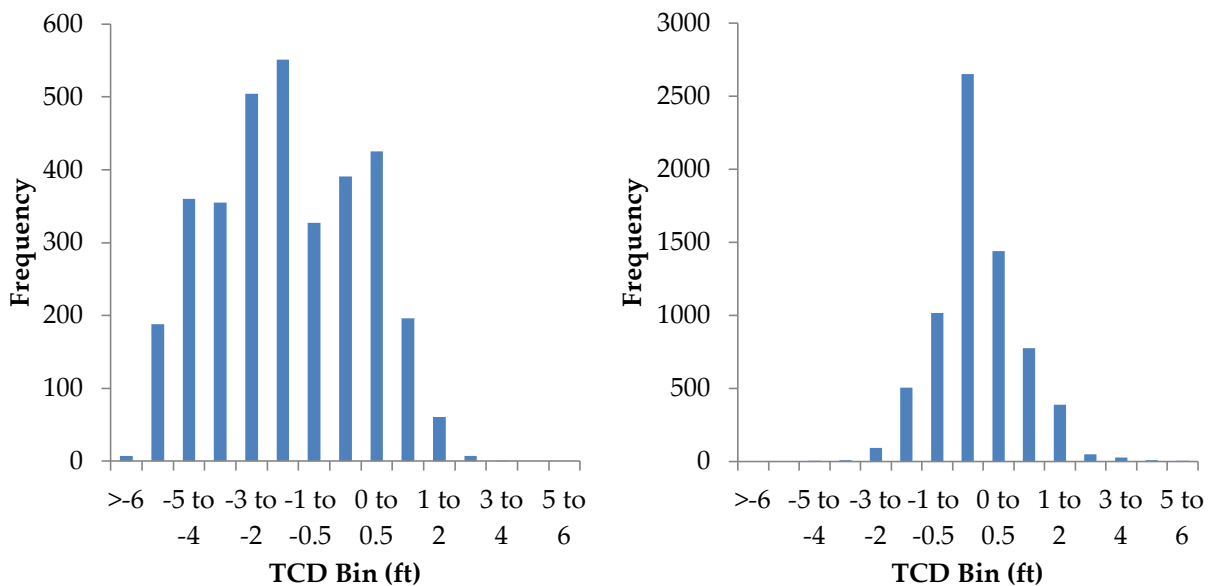


**Figure 11. Elevation change histogram for the upstream area (left) and downstream area (right) for the Fall 2012 to Summer 2013 epoch.**

### 5.3.2. 2007 to Summer 2013 TCD

To evaluate the overall status of EDR from 2007 to the summer of 2013 an additional TCD analysis was done for the period spanning 2007 to the summer of 2013. For the upstream area this analysis predicted 196 tons of erosion and 1,322 tons of deposition (Table 6). In addition, 241 tons of deposition was predicted using aerial photographs,

so the net change was 1,368 tons. The patterns of deposition show that the cobble bar below the USGS gaging station is accreting on the inside face (Figure 12). Additional deposition also occurred in the center of the channel, likely in between large boulders and existing bed material where it can get trapped. Erosion was focused on river, opposite of the cobble bar. Histograms show that deposition and erosion were mostly low magnitude, dominating the 0 to 0.5 foot and -0.5 to 0 foot bins, respectively (Figure 14). Approximately 50 and 75% of erosion was less than 0.65 and 0.35 ft, respectively. For deposition, approximately 50 and 75% were less than 1 and 0.5 ft, respectively.

For the downstream area TCD analysis predicted 4,535 tons of deposition and 1,303 tons of erosion. Using prior areas of deposition gleaned from the imagery, there was an additional 1,477 tons of deposition (Table 6). The downstream patterns of channel change are overall very coherent, with deposition following a central band through the river except at the constricted riffle chute, which has been consistently eroding since monitoring commenced (Figure 13). Similar to the upstream area, the histogram shows that deposition and erosion were mostly low magnitude, dominating the 0 to 0.5 ft and -0.5 to 0 ft bins, respectively (Figure 14). Approximately 50 and 75% of erosion was less than 0.65 and 0.25 ft, respectively. For deposition, approximately 50 and 75% were less than 1.2 and 0.65 ft, respectively.

**Table 6. Upstream and downstream volumes of erosion and deposition for the 2007 to Summer 2013 epoch**

	Upstream			Downstream		
	Erosion (tons)	Deposition (tons)	Net (tons)	Erosion (tons)	Deposition (tons)	Net (tons)
2007 - 2013 Summer	-196	1322	1126	-1303	4535	3233
Images/RTK	NA	241	241	NA	1477	1477
Net	-196	1563	<b>1367</b>	-1303	6012	<b>4710</b>
Total Change (erosion + deposition)			1760	7,315		

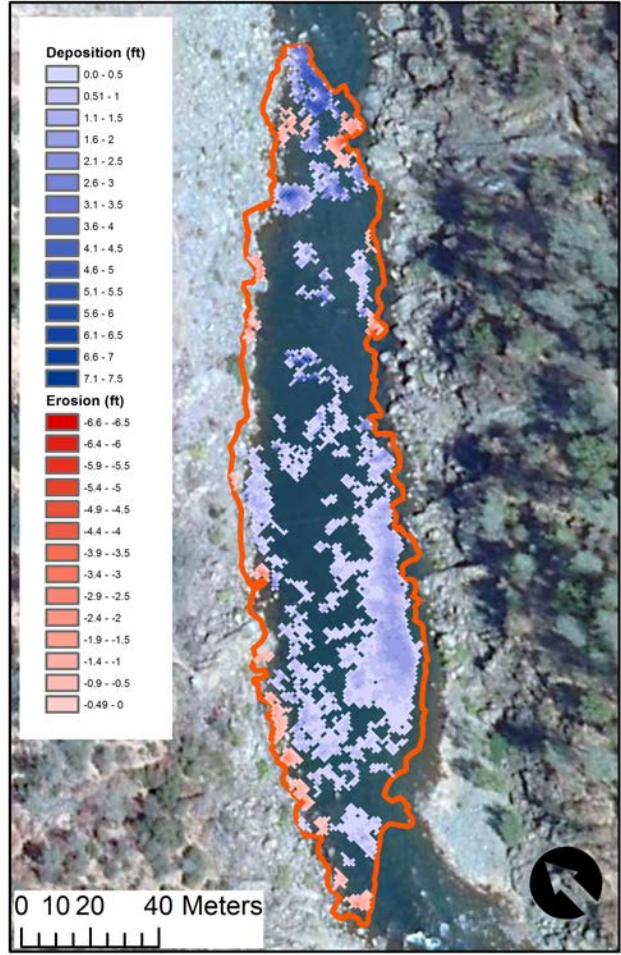


**Figure 12. Upstream injection area patterns of erosion and deposition for the 2007 to Summer 2013 epoch at the 95% confidence limit.**

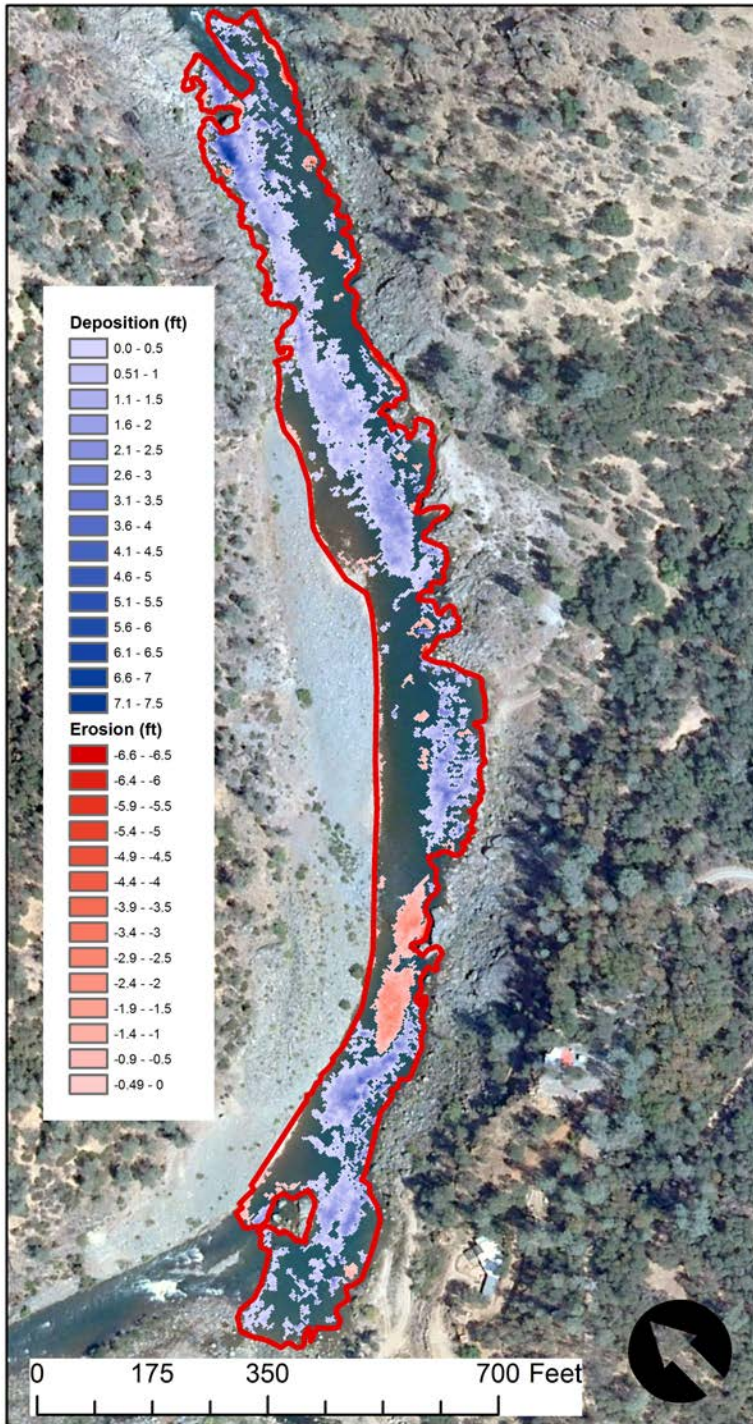


**Figure 13. Downstream area TCD predicted patterns of erosion and deposition for the 2007 to Summer 2013 epoch at the 95% confidence limit.**

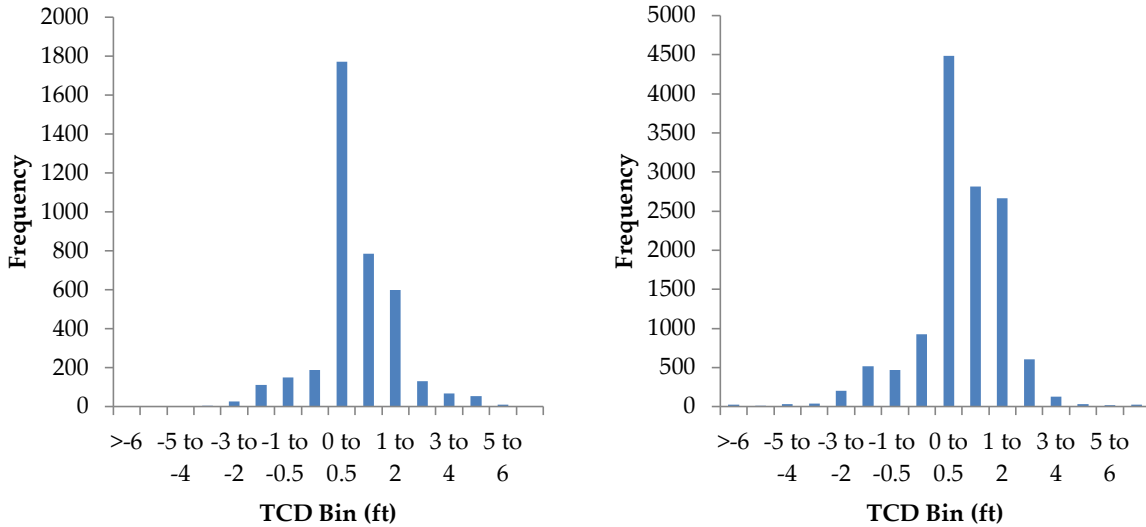


**Figure 14. Elevation change histogram for the upstream area (left) and downstream area (right) for the 2007 to summer 2013 epoch.**

## 5.4. Sediment Budgeting

### 5.4.1. Sediment Budget for Fall 2012 to Summer 2013

Overall, the dominant response of the 2012 project to the late fall atmospheric river flood was erosion of placed material in the upstream area and deposition in the downstream area. Secondarily, there was some storage (deposition) in the upstream section on river left at the cobble point bar and in the boulders and bedrock in the center of the channel before the crest of the rapid. Both erosional and depositional responses were corroborated by the TCD and image analysis. For the downstream area, a large depositional band formed that terminated approximately midway through the downstream TCD area. Erosion was also predicted along the edges of the channel, especially adjacent to protruding bedrock obstructions. Next, sediment budgets are estimated for the upstream and downstream areas.

To perform a sediment budget for the upstream area for the fall 2012 to summer 2013 epoch, both erosion and deposition are considered from the TCD and image analysis yielding 3,901 tons accounted for (Table 5). The fill from the 2012 gravel injection project detected from a previous TCD analysis was 3,908 tons and an addition 874 tons were detected from imagery yielding 4,782 tons. Comparing this with the TCD predicted channel change for fall 2012 to summer 2013 epoch 82% of the material was accounted for. These values compare rather well to the 88% accounted for during the 2011-2012 period. Because the riverbed is so complex and rough with boulders and

bedrock protrusions, it is very difficult to fully close the sediment budget, even with the very detailed bathymetric that is being done.

The next step in this sediment budget was to determine how much material actually made it to the downstream area. For this, the net TCD predicted change of 3,227 tons is considered, which accounts for both the deposition and erosion that occurred in the upstream area. Given the amount of 4,782 tons that was detected in the river during the prior injection period, 1,555 tons were exported to the downstream area. For the downstream area the TCD and image analysis predicted that 1,085 tons were deposited and also that 1,116 tons were eroded, with a net loss of 31 tons. The amount of predicted deposition was 70% of what was determined to be exported downstream. The remaining 30% or ~470 tons could be associated with (1) deeper fill depths than the 0.18 ft assumed for image and RTK deposits, (2) material losses in the angular bed of the river, and (3) material trapping in the cobble bar just above the rapid, which is excluded from the TCD analysis. As a final remark, the unaccounted material could imply that there was export to the Narrows, but it is unlikely that what was injected in 2012 made it through the entire EDR, given the short storm duration. Scouting trips through the Narrows have not found major deposits there coming out of EDR. Google Earth imagery taken in May of 2013 shows one sizable gravel/cobble bar that was already known to be a spawning site in recent years of surveys by the Yuba Accord River Management Team and it may be receiving some sediment is leaving the EDR and replenishing this location in the Narrows. However, it is most likely that the majority of the missing material simply filtered into the vast porosity of the highly complex and rough boulder bed.

#### **5.4.2. Overall Sediment Budget from 2007-2013**

At this point it is useful to assess the total amount of topographic change from the 2007 baseline period to the summer of 2013. Not including the ~350 tons added in 2007, ~ 2 injections of 5,000 tons occurred, so roughly 10,000 tons have been added to the river (subsequent to this study a third injection of another ~ 5,00 tons was done in fall 2013, but that is not investigated herein). For the two major injections covered by this report that have been mobilized by the river, the amount found in the river after each one using TCD and image analysis was 4,010 and 4,782 tons, respectively.

Taking the net upstream and downstream volumes of deposition the TCD and image analyses accounted for 7,569 tons of gravel. Given that prior analyses reported 8,792 tons of gravel being added to the river, 86% has been accounted for. The remaining 14% (e.g. 1,223 tons) is thought to be dispersed through EDR in the bed porosity and too sparse or too covered to be detected by imagery. The fall 2011 to fall 2012 TCD analysis

in Brown and Pasternack (2013) suggested that approximately 400 tons left the EDR. Further, 77% of the erosion that occurred in the fall 2012 to summer 2013 epoch was associated with prior deposition so the remaining 33% or 368 tons also likely left the EDR. This accounts for 768 tons, so the remaining 455 tons also left the Narrows or is still in the EDR but was undetected. Regardless, the TCD and image analysis shows that a very good percentage of the gravel added to the EDR, 86%, has been accounted for.

## **6.0 The Role of Deer Creek on Sediment Storage in the EDR**

The Deer Creek confluence has been anecdotally reported as having a unique hydraulic impact on the Yuba River from local landowner, Ralph Mullican. For example, during some of the largest storms Mr. Mullican has reported Deer Creek essentially forming a jet that impacts the bedrock wall on river right and in some cases pointing somewhat upstream. Because the Narrows has never been mapped it is difficult to assess the interplay between channel hydraulics in the Yuba and the timing of flood peaks between the two. Deer Creek is a smaller basin and due to its elevation is primarily a rain driven system. The Yuba River is obviously much larger and its hydrology can be driven by both rain and snow events.

To analyze the flood timing between these two, we compiled hydrologic time series for flow gages on the Yuba River (cdec.gov; 'yrs') and Deer Creek (cdec.gov; 'dcs') and examined the temporal peaking of the two gages for the 2005/2006 "New Years' Eve" storm and the floods evaluated in this report (Figs. 15,16). For the 2005/2006 "New Years' Eve" storm Deer Creek peaked at 12,300 cfs as 10am, while the Yuba River peaked two hours later at 96,100 cfs (Figure 15). When Deer Creek peaked, however, flow in the Yuba was still very high at 92,800 cfs. During the November and December atmospheric river storms of 2012, Deer Creek also peak before the Yuba River (Figure 16). On December 2, 2012 at 11am Deer Creek peaked at 12,800 cfs while the Yuba River was flowing at 12,871 cfs and beginning to rise. By 3 pm when the Yuba River peaked at 30,877 cfs Deer Creek had already receded to 3,720 cfs. Therefore, from analyzing these two events it appears that Deer Creek does indeed typically peak before the Yuba River by a few hours.

With knowledge of how the Yuba River and Deer Creek interact, several hydrologic and hydrodynamic scenarios are possible that may affect sediment routing from the EDR to the Lower Yuba River. Hydrologically, the two watercourses can peak synchronously or asynchronously. For the latter either one could peak first, although it appears that Deer Creek commonly leads the Yuba due to the smaller drainage area and lower elevation of the watershed. While the timing of peak floods is important it is also possible that local hydrodynamics can play a major role in whether Deer Creek shields gravel transport from the EDR into the Narrows reach. A sediment transport buffer

effect can occur whereby the Deer Creek confluence produces a hydrodynamic jet that effectively creates a “gravel curtain” that prevents material from leaving the EDR and going into the Narrows.

The flow hydrodynamics at the Deer Creek confluence, along with tailwater conditions in the Yuba River, are important controls on whether or not a hydrodynamic jet creates a sediment transport buffer. To create a buffer for upstream sediment transport there needs to be either a cross-stream or upstream jet from Deer Creek that impinges into the main flow of the Yuba River, either at a right angle or even pointed upstream. When Deer Creek is flowing deep and fast it can effectively jump out of the downstream oriented channel on the fan following a straight line impinge the bedrock wall on river left of the Yuba River. In this case Deer Creek has to have greater flow momentum than the Yuba River so that it can effectively short circuit any downstream sediment transport. When tailwater conditions in the Yuba River are high, Deer Creek could also have an upstream orientation as discussed by Mr. Mullican. Given the dramatic constriction in the Narrows it is possible that a large backwater does occur during large events. If Deer Creek peaked during such a backwater it is possible that flow could be oriented upstream or perpendicular to the Yuba. If the Yuba is backwatered and Deer Creek does not have substantially deep and fast flow it is likely that the Yuba would push the incoming Deer Creek flow downstream. In summary, there are a lot of different combinations of flow hydrology and hydrodynamics that can occur and it is possible that Deer Creek can enhance sediment storage in the EDR.

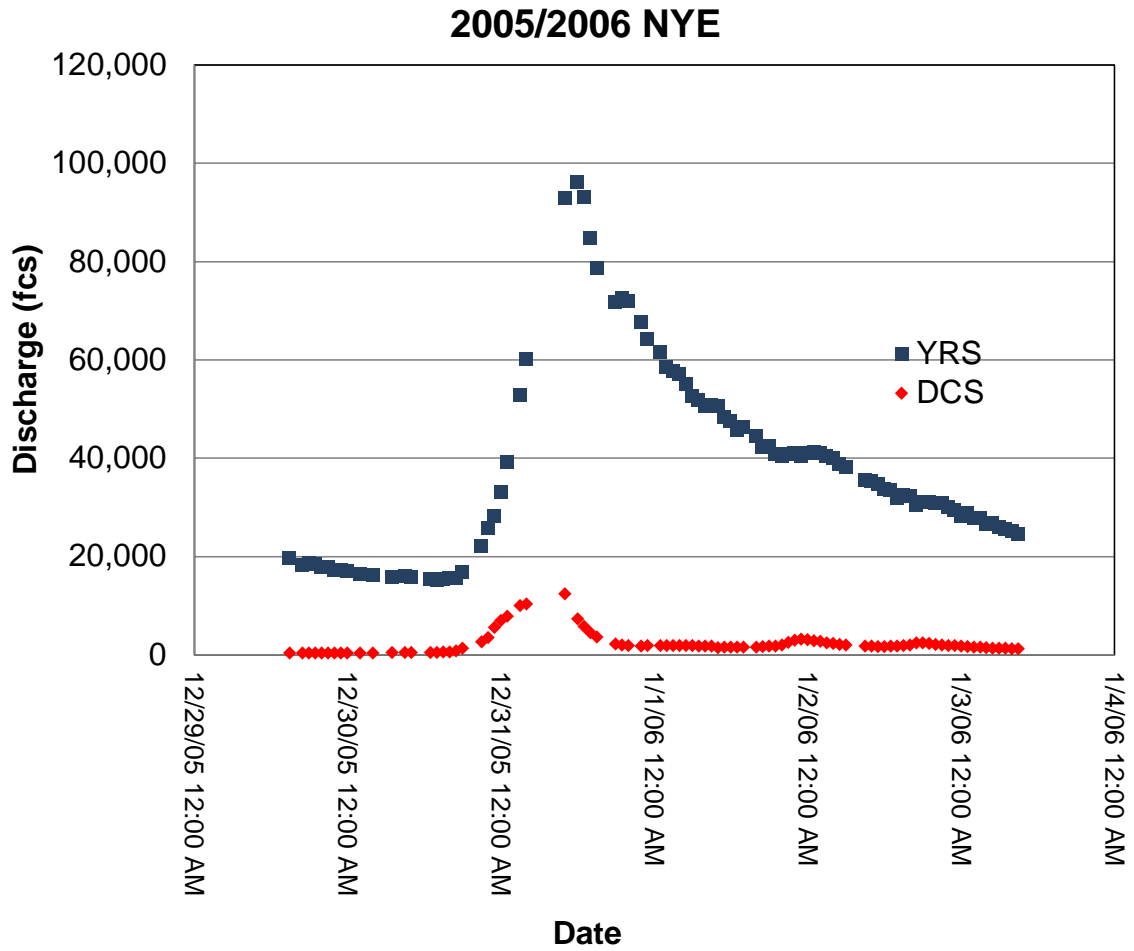


**Figure 15. Hydrographs of the Yuba River at the Smartsville gage (YRS) and for Deer Creek (DCS) for the 2005/2006 NYE storm.**

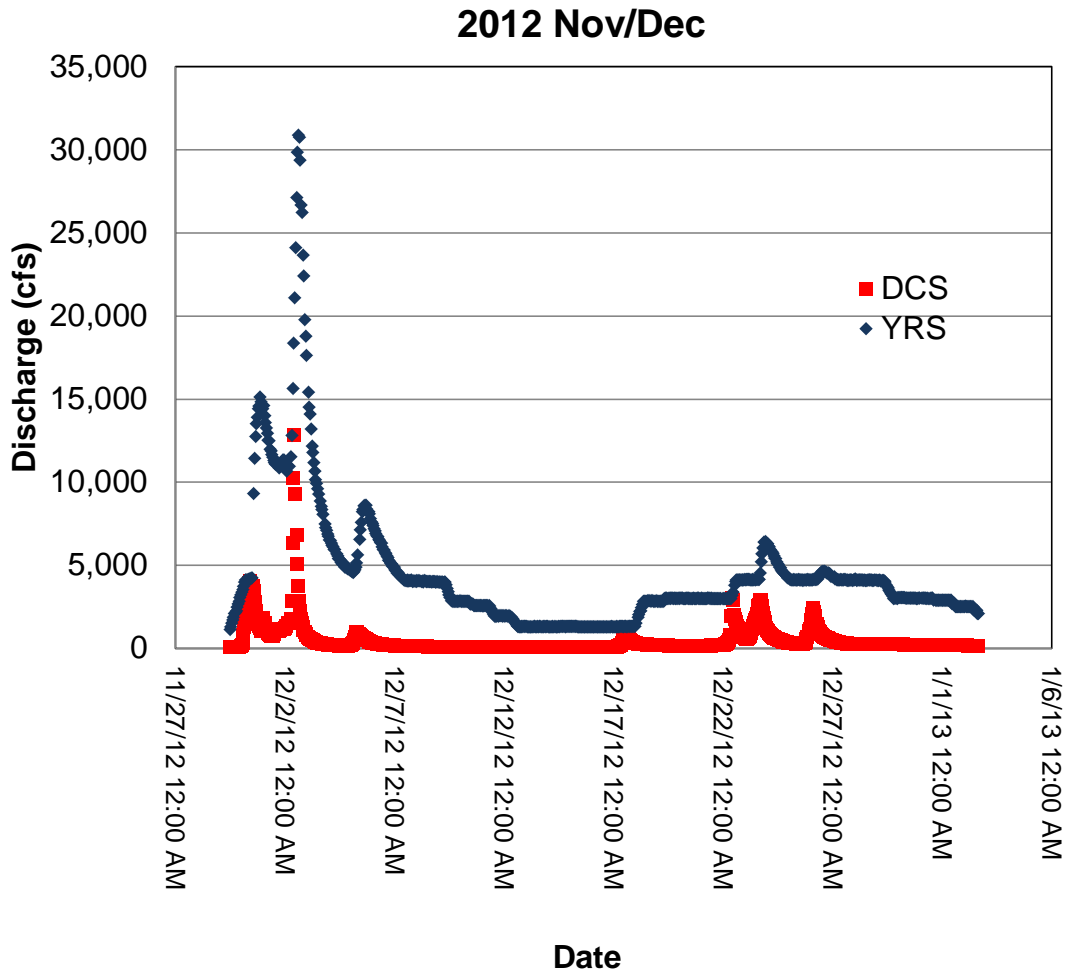


**Figure 16. Hydrographs of the Yuba River at the Smartsville gage (YRS) and for Deer Creek (DCS) for the atmospheric river floods of Nov./Dec. 2012 studied in this report.**

## 7.0 Conclusions

The atmospheric river storms that occurred in November and December of 2012 produced two peak discharge events in the EDR that were above the bankfull flow of 5,000 cfs. Only the first storm, which peaked at over 30,000 cfs was of sufficient magnitude to effect channel change in the EDR. TCD and sediment budgeting analyses predicted that erosion of the 2012 gravel injection project with some material remaining upstream. Sediment budgeting and TCD analyses accounted for 82% of the sediment that was injected upstream during the summer of 2012. In the downstream area, both erosion and deposition occurred. Erosion was primarily focused towards the bottom half of the downstream section and 77% of areas that eroded were areas of prior gravel deposition. Deposition was focused in the upper half of the downstream section where

it is thought that the first atmospheric river storm transported material before flows receded. It is concluded that single flood events can route gravel deposits a modest distance, but the flood analyzed herein did not route any of the 2012 injection out of the EDR. It appears that most of the sediment injected made it to just above Sinoro Bar.

Sediment budgeting for 2007 to the summer of 2013 accounted for 86% (7,625 tons) of the two gravel augmentation projects that have occurred to that point in time. Overall, widespread deposition in the channel has occurred, but some material is likely leaving the EDR, even though we can find no deposits to show that. For example, erosion for the fall 2012 to summer 2013 epoch showed that material that had previously deposited in 2011 and 2012 eroded and entered the Narrows reach. There has been one zone of consistent erosion, a chute at the bottom of a riffle towards the end of the reach has appears to be head-cutting into the upstream riffle. At least 768 tons has left the EDR and a remaining 455 tons may have left or is present in areas not included in or undetectable from the TCD and image analyses.

The primary objective of the GAIP is to add gravel that can be dispersed downstream of the initial injection area and create habitat throughout the EDR. The gravel injection site is at a very narrow constriction in the river, and by design gravel placed there is intended to move downstream throughout EDR to create new deposits. Since the beginning of the implementation of the GAIP, a notable amount of gravel and cobble has accumulated in the EDR, but there is still a long way to go before the reach has filled to its estimated storage capacity. In years when flows are low after gravel addition, then a large coherent spawning site will be available to use in the injection zone, but this should not be expected to be sustainable; it is a short-term bonus. All GAIP monitoring studies have observed and quantified the downstream transport of injected gravels and the positive effects it has had on creating salmon spawning habitat throughout the reach.

Inevitably, sediment will leave EDR, and indeed some has now been observed to do so, but still very little. According to natural law, transport of any constituent is proportional to its abundance, so it is anticipated that as the total amount of sediment stored in the EDR increases, the absolute amount of sediment exported out of it will increase as well. The geomorphic goal of the GAIP is to build up the sediment storage in the reach even as export will occur and grow with storage. Once the reach has achieved its storage goal, then further additions need only balance export losses.

The EDR canyon in the region where Sinoro Bar is located is wide, but because of shot rock deposition and mechanized in-channel mining that channelized this section of the river, added river-rounded gravels are now routing in a river that is fairly constrained in this region. The opportunity remains for someone to rehabilitate the river in the vicinity of Sinoro Bar, and then the gravel and cobble being added to the river by the

Corps could yield even greater benefits in holistic combination with such a site-specific rehabilitation downstream of the injection site.

## 8.0 References

- Brown, R.A. and Pasternack, G.B. 2012. Monitoring and assessment of the 2010-2011 gravel/cobble augmentation in the Englebright Dam Reach of the lower Yuba River, CA. Prepared for the U.S. Army Corps of Engineers, Sacramento District. University of California at Davis, Davis, CA.
- Brown, R.A. and Pasternack, G.B. 2013. Monitoring and assessment of the 2011-2012 gravel/cobble augmentation in the Englebright Dam Reach of the lower Yuba River, CA. Prepared for the U.S. Army Corps of Engineers, Sacramento District. University of California at Davis, Davis, CA.
- Carley, J. K., Pasternack, G. B., Wyrick, J. R., Barker, J. R., Bratovich, P. M., Massa, D. A., Reedy, G. D., Johnson, T. R. submitted. Accounting for uncertainty in topographic change detection between contour maps and point cloud models. *Geomorphology*.
- Heritage, G.L., Milan, D. J., Large, R.G., Fuller, I.C. 2009. Influence of survey strategy and interpolation model on DEM quality. *Geomorphology* 112, 334-344.
- Lowe, D.G. 2004. Distinctive image features from scale-invariant keypoints. *International Journal of Computer Vision* 60 (2), 91-110.
- Pasternack, G. B. 2009. Current Status of an On-going Gravel Injection Experiment on the Lower Yuba River, CA. Prepared for the U.S. Army Corps of Engineers.
- Pasternack, G. B. 2010. Gravel/Cobble Augmentation Implementation Plan (GAIP) for the Englebright Dam Reach of the Lower Yuba River, CA. Prepared for the U.S. Army Corps of Engineers.
- Wheaton JM, Brasington J, Darby SE and Sear D. 2010a. Accounting for Uncertainty in DEMs from Repeat Topographic Surveys: Improved Sediment Budgets. *Earth Surface Processes and Landforms*. 35 (2): 136-156. DOI: 10.1002/esp.1886
- Wheaton JM, Brasington J, Darby SE, Merz JE, Pasternack GB, Sear DA and Vericat D. 2010b. Linking Geomorphic Changes to Salmonid Habitat at a Scale Relevant to Fish. *River Research and Applications*. 26: 469-486. DOI: 10.1002/rra.1305.